Birth and Morphological Evolution of Step Bunches under Electromigration

J. Chang, O. Pierre-Louis, and C. Misbah
Spectro, UJF-Grenoble 1, BP87, F38402 Saint Martin d'Hères, France
(Received 15 November 2005; published 16 May 2006)

We analyze the dynamics of electromigration-induced step bunching in the absence of desorption. We show that, even when the instability occurs at long wavelength, hinting to a smooth morphology, the surface suddenly splits into bunches escorted with wide terraces, in agreement with several observations. As the size of the bunches increases, a nonstandard regime is exhibited, namely, the bunches do not match tangentially to the facet, as would the classical Pokrosvky-Talapov shape dictate. This Letter presents a complete scenario of evolution of bunches from their birth up to their ultimate stage.

DOI: 10.1103/PhysRevLett.96.195901 PACS numbers: 66.30.Qa, 05.70.Ln, 36.40.Sx, 68.35.Fx

Stepped surfaces constitute a subject of intensive research both theoretically and experimentally. The reasons are at least twofold: (i) they constitute an interesting and rich system of nonequilibrium statistical mechanics which continues to be a source of many puzzles, (ii) they are viewed as promising templates for the design of novel architectures at the nanoscale. A persistent behavior on stepped surfaces under nonequilibrium conditions is the breakdown of the regular vicinal surfaces into a coexistence of bunches of steps and terraces. One of the major studied issues is step bunching triggered by electromigration [1,2]. Electromigration offers an attractive tool to monitor in a rather controlled fashion the surface evolution. In addition, it has led to a surprisingly complex picture of evolution both for open and closed systems [3–9]. A full understanding of the intricate dynamics still continues to pose a formidable challenge, however. For example, while it can be proved from thermodynamical considerations that the bunch profile must match tangentially to a facet, this is not *a priori* obvious under nonequilibrium conditions. Furthermore, if the (experimentally relevant for silicon) asymptotic regime of bunches has achieved a mature level of understanding [4,9], the same cannot be said about the full evolution starting from the initial birth of instability. This evolution is accessible to experiments, and thus its analysis should bring new views on the ingredients and phenomena that underlie surface pattern evolution. The present study focuses precisely on these issues.

By analyzing an initially stepped regular surface, in the simplest configuration where only electromigration drives the dynamics, we are able to provide the evolution scenarios from the instability birth until the ultimate stage of evolution. More precisely, in the limit where the migration force is small, the major steps reported on here are: (i) the instability initially develops as long wavelength and continuous step density waves. By means of a nonlinear expansion, we show that the amplitude of these waves increases while their wavelength is frozen. (ii) With the increase of the amplitude, the step density locally reaches zero. This indicates the opening of wide terraces which are free of steps, where the continuum description breaks down, connected by smooth step bunches where the continuum approach still holds. (iii) The occurrence of wide terraces as time elapses needs a mixed treatment where bunches are treated in the continuum limit while facets require a separate analysis. With the help of an asymptotic matching we show that the bunch profile does not match tangentially to the facet. We find that several scaling regimes are explored in the course of time. We finally discuss the existing theoretical and experimental literature in the light of our results.

Step model.—We outline the step model, following the same lines as Ref. [10]. We consider a one-dimensional vicinal surface along the x coordinate. On terraces, mobile atoms diffuse with a diffusion constant D, and are subject to a drift velocity v (>0 for a downhill drift). Mass conservation on terraces then reads, within the quasistatic approximation:

$$0 = D\partial_{xx}c - \frac{D}{\xi}\partial_x c, \tag{1}$$

where $\xi = D/v$. At the steps, we assume kinetic boundary conditions:

$$D\partial_x c_\pm - \frac{D}{\xi}c_\pm = \pm\frac{D}{d}(c_\pm - c_{\mathrm{eq}}), \tag{2}$$

where d is the attachment-detachment kinetic length. The local equilibrium concentration in the vicinity of the nth step is then obtained via a linearized Gibbs-Thomson relation: $c^n_{\mathrm{eq}} = c^0_{\mathrm{eq}}[1 + A(l_n^{-3} - l_{n+1}^{-3})]$ where we have assumed the usual interstep repulsion which costs an energy $\sim 1/l^2$ between neighboring steps. The concentration on terraces is calculated from Eqs. (1) and (2). Mass conservation at the steps $V_n = \Omega[D\partial_x c - Dc/\xi]^+_-$, where Ω is the atomic area, then provides us with the velocity of the nth step $V_n = j_n - j_{n-1}$, where

$$j_n = \Omega D\frac{(c^{n+1}_{\mathrm{eq}} + c^n_{\mathrm{eq}})/2\xi + (c^{n+1}_{\mathrm{eq}} - c^n_{\mathrm{eq}})/\mathcal{L}_n}{1 + d/\mathcal{L}_n}, \tag{3}$$

with $\mathcal{L}_n = 2\xi\tanh(l_n/2\xi)$.

Linear stability analysis.—We first perform a linear stability analysis. To do so, we can consider a single Fourier mode: $\zeta_n(t) = \zeta_{\omega\phi} \exp(i\omega t + in\phi)$, having a spatial wavelength $\lambda = 2\pi l/\phi$. Linearizing Eq. (3), we obtain a dispersion relation relating $i\omega$ to ϕ. The real part of $i\omega$ accounts for stability. We find that the train of steps is unstable for $\xi > 0$. We consider the experimentally relevant limit $\xi \gg l$. In the weak-migration limit $1/\xi \ll 6A(l+d)/dl^4$, the instability appears at ϕ small, i.e., at long wavelengths. The period of the most unstable mode is:

$$N_m = 2\pi[6A\xi\bar{\rho}^3(\bar{\rho} + 1/d)]^{1/2}, \tag{4}$$

where $\bar{\rho} = 1/l$ is the average step density. The corresponding wavelength along x is simply defined as: $\lambda_m = N_m/\bar{\rho}$. For Si(111) at 900 °C, one has $\xi \sim 10^7$ Å, $A \sim 10$ Å^3, and $d \gg l$. Therefore, long wavelength bunching occurs for $l < 10^2$ Å, which corresponds to experiments of Ref. [11]. Long wavelength bunching can also be obtained from a decrease of the average migration force (i.e., an increase of ξ) by means of a high frequency ac electric current.

It is only when we consider situations far from the threshold, when $1/\xi \gg 6A(l+d)/dl^4$, that the most unstable mode happens to be the pairing mode $\phi = \pi$. Pairs of steps then form initially, which again merge together to form bigger and bigger bunches of steps. This scenario was called hierarchical bunching in Ref. [4].

Nonlinear dynamics. (1) step density waves.—We first show the initiation of a long wavelength smooth oscillation of the step density, which breaks down then into well-separated bunches. The situation is similar to that of step meandering without desorption [12]: dynamics is highly nonlinear (due to the coincidence between instability threshold and lack of equilibrium [13]) for weak migration. The obtained evolution equation is $\partial_t \zeta = a\partial_y j$, with:

$$j = \frac{\Omega D c_{\mathrm{eq}}^0}{1 + d\rho}\left(\frac{1}{\xi} - aA\rho\,\partial_{yy}\rho^3\right), \tag{5}$$

where y is the surface height, $\rho = 1/a\partial_y x = 1/(l - a\partial_y\zeta)$ is the local step density. We seek steady solutions of Eq. (5) in the form $j = J$ where J is an unknown constant. From Eq. (5), the dynamics of ρ is invariant under the $y \to -y$ symmetry. Terms which break this symmetry are encountered at higher orders in the expansion. Therefore, there is no global drift of the bunch. Integrating $J(1/\rho + d)$ along y on a distance Na, we find

$$\frac{J}{\Omega D c_{\mathrm{eq}}^0}(W + Nd) = \frac{W}{\rho\xi} + A(\rho_+^3 - \rho_-^3), \tag{6}$$

where $\rho_\pm$ is the value of ρ at the boundaries of the integration domain, and W is the width of the integration domain along x. If integration is performed over one period, then we have $\rho_+ = \rho_-$ and $N/W = \bar{\rho}$. Finally,

$$J = \frac{\Omega D c_{\mathrm{eq}}^0}{1 + d\bar{\rho}}\,\frac{1}{\xi}, \tag{7}$$

which generalizes the law derived in Ref. [9] from a phenomenological argument in the limit where d is large.

The equation $j = J$ can be rewritten in a form which describes the motion of a fictitious particle in "time" y: $a^2 A\partial_{yy}u = -d\mathcal{V}/du$, with the potential

$$\mathcal{V}(u) = \frac{Jd}{\Omega D c_{\mathrm{eq}}^0}u - \frac{3}{2}\left(\frac{1}{\xi} - \frac{J}{\Omega D c_{\mathrm{eq}}^0}\right)u^{2/3}, \tag{8}$$

where $u = \rho^3$. Periodic steady states are the oscillatory solutions in the potential $\mathcal{V}$ shown in Fig. 2. Their period N_s takes the form $N_s(\bar{\rho}l_0) = N_m f(\bar{\rho}l_0)$, where l_0, the largest terrace within a period is defined from the relation $l_0 = 1/\rho_{\min}$, where $\rho_{\min}$ is the smallest step density within the period. The function f is defined as

$$f(\bar{\rho}l_0) = \int_{\theta_0}^{\pi} \frac{d\theta \sin(\theta)}{4\pi 3^{1/2}}\left[\frac{1}{c - 1/2} - \frac{1}{\bar{c} - 1/2}\right], \tag{9}$$

where $c = \cos(\theta/3)$, $\bar{c} = \cos(\theta/3 - 2\pi/3)$, and $\theta_0 = \pi/2 + 3\arcsin(\bar{\rho}l_0 - 1/2)$. The function f decreases monotonously from $f(\bar{\rho}l_0 = 1) = 1/\sqrt{2}$ for perturbations of small amplitude, to $f(\bar{\rho}l_0 \to \infty) = \sqrt{3}/\pi$ for the largest amplitude when the minimum step density approaches zero. Therefore, $f(\bar{\rho}l_0) < 1$, and all steady-state bunch sizes are smaller than that of the linearly most unstable mode $N_s(\bar{\rho}l_0) < N_m$. From the study of Refs. [12,14] we conclude that coarsening does not occur, and the wavelength should be frozen while the amplitude of the step density wave increases, up to the maximum possible amplitude, for which $l_0 \to \infty$. Hence, large terraces should form at zero density, which indicates a transition from continuous step density waves to bunches separated by large terraces. This scenario is confirmed by the numerical solution of Eq. (5) which reveals the formation of cusps (at small ρ). The numerical solution of (3) for ξ large corroborates the previous analysis, as shown in Fig. 1. Indeed, the vicinal surface suddenly splits into bunches bounded by large terraces. Moreover, the $y \to -y$ symmetry of the dynamics is observed.

Nonlinear analysis. (2) Bunches connected by wide facets.—Since wide terraces appear, the continuum description of the surface profile should break down and a more careful study is needed as presented below. We can tackle this question by resorting to a semicontinuous (or mixed) approach, where isolated terraces are treated as they are, while bunches are described in the continuum limit. The matching to a large terrace of width l_0 is based upon the use of (3). In the vicinity of the facet from the bunch side a continuum limit is legitimate, and boundary conditions are obtained in the limit $l_0 \ll \xi$:

$$u_e = -[Jd/\Omega D c_{\mathrm{eq}}^0 + (J/\Omega D c_{\mathrm{eq}}^0 - \xi^{-1})l_0]/(2A), \tag{10}$$

$$\partial_y u_e = u_e - [Jd/\Omega D c_{\mathrm{eq}}^0 + (J/\Omega D c_{\mathrm{eq}}^0 - \xi^{-1})u_e^{-1/3}]/A, \tag{11}$$

where $u = \rho^3$. The subscript in u_e stands for "edge."

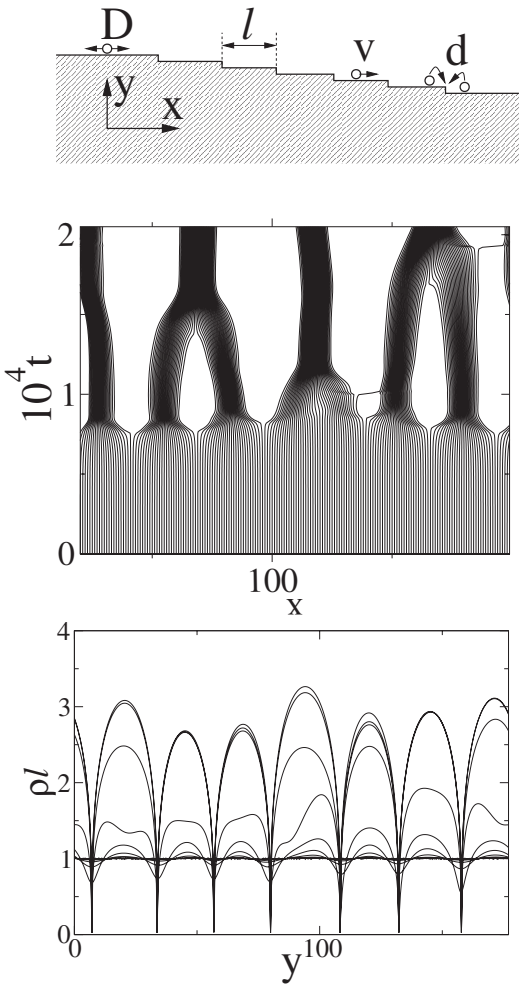

FIG. 1. Upper panel: Sketch of a vicinal surface. Middle panel: Numerical solution of the dynamics for a train of 200 steps with periodic boundary conditions. x is the step position, and t is the time. Lower panel: Solution of the highly nonlinear equation. Step density ρ as a function of y at different times.

Inside the bunch, the profile obeys Eq. (8). Finding the periodic steady states is now equivalent to solving Eq. (8) with the boundary conditions (10) and (11). The novel feature lies in the nontangential matching at the facet described by (11). Note that in the absence of a driving force ($\xi^{-1} = 0$ and $J = 0$), u_e vanishes and so does $\partial_y u_e$. We recover the tangential matching of Pokrovsky-Talapov. Finally, the conservation of the number of steps leads to an additional constraint: $N = a\bar{\rho}(W + l_0)$.

The above set of equations reveal several regimes. First, when $\lambda_m = N_m/\bar{\rho} \ll l_0 \ll \xi$, one finds that $N = \bar{\rho} l_0$ and that the flux still obeys relation (7). For this regime, referred to as regime I, we obtain the relations reported in Table I. The slope at the edge increases with the bunch size, but is much smaller than the maximum slope: $l_e^{-1} \sim N^{1/3} \ll l_{\min}^{-1} \sim N^{2/3}$. These scalings were already mentioned in Refs. [4,15].

In the limit of very large bunches $l_0 \gg \xi$, boundary conditions similar to Eqs. (10) and (11), are once again extracted from the steady state of Eq. (3). We now have

$$u_e = (1 - J\xi/\Omega D c_{\mathrm{eq}})/A, \tag{12}$$

while Eq. (11) is unchanged. We have identified 4 regimes. We only report on two asymptotic cases, however. These correspond to the smallest and the largest bunches. In the first limit, we obtain regime II, which is similar to I, especially regarding the dependence with N, as shown on Table I. Furthermore, deviations from relation (7), which relies on the assumption that the terrace width is smaller than ξ, are reported in Table I. The large bunch limit, denoted as regime III, is also reported on Table I. In this limit the term $J \sim N^{-1/2}$ in Eq. (12) is negligible, so that the slope at the edge $l_e^{-1} = u_e^{1/3} = A^{-1/3}$ is large. Using orders of magnitude valid for Si(111) [2], we find that $N \gg \xi^{3/2} A^{-1/2}$ implies $N \gg 10^{12}$, which is too large. Therefore, this regime is not accessible to Si(111) experiments. Moreover, the width of the last terrace $l_e = A^{1/3}$ is of the order of an atomic distance. Whether or not there are other systems for which this behavior becomes relevant requires the knowledge of several physical parameters which are not presently available.

Discussion and conclusion.—Several remarks are in order. (i) Once separate bunches are formed, the dynamics is similar to that observed for hierarchical bunching [4]. (ii) The scaling laws of regimes I and II have been reported on in the literature [9,10] without using the appropriate boundary conditions (10) and (11). It must be emphasized, however, that the boundary conditions at the facet edge do not only change the prefactors of the scaling laws, but also the scaling itself, as shown above from the difference between regimes I and III. For example, our result is improved as compared to Ref. [4], which has considered the fast kinetics limit $d \ll \bar{\rho}^{-1}$. We have checked that our results of regime I provide a numerical fit to the simulations of a steady bunch in a periodic box in Ref. [4], which

TABLE I. Scaling regimes for step bunches.

Regime	I: $l_0 \ll \xi$	II: $l_0 \gg \xi$ $N \ll \xi/d$; $\xi(d/A)^{1/2}$	III: $l_0 \gg \xi$ $N \gg \xi^{3/2}A^{-1/2}$; $(A\xi)^{1/2}d^{-2}$
W	$b\bar{\rho}^{-1}N_m^{2/3}N^{1/3}$; $b \approx 0.27$	$b_1 A^{1/3}\xi^{1/3}d^{-1/3}N^{1/3}$; $b_1 \approx 2.05$	$2^{1/2}(A\xi)^{1/4}N^{1/2}$
$l_{\min}$	$\pi^{-2/3}3^{-1/3}\bar{\rho}^{-1}N_m^{2/3}N^{-2/3}$	$2^{2/3}A^{1/3}\xi^{1/3}d^{-1/3}N^{-2/3}$	$2^{3/2}3^{1/4}(A\xi)^{1/4}N^{-1/2}$
l_e	$\pi^{-2/3}12^{-1/3}\bar{\rho}^{-1}N_m^{2/3}N^{-1/3}$	$A^{1/3}\xi^{1/3}d^{-1/3}N^{-1/3}$	$A^{1/3}$
J	$\Omega(Dc_{\mathrm{eq}}/\xi)/(1 + d\bar{\rho})$	$\Omega(Dc_{\mathrm{eq}}^0/\xi)(1 - dN/\xi)$	$\sim N^{-1/2}$

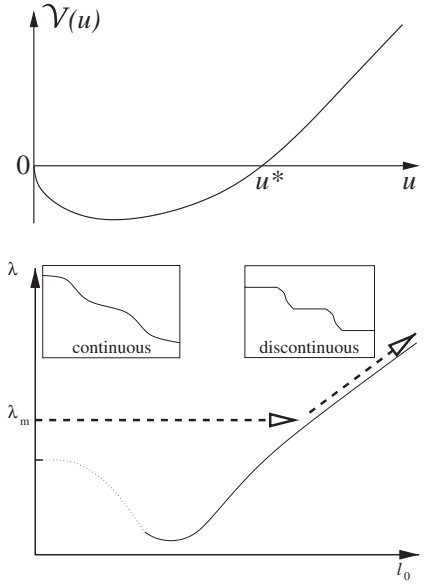

FIG. 2. Upper panel: Potential $\mathcal{V}$. The continuous steady state are oscillations between 0 and u^*. Solutions I and II explore the linear part at $u > u^*$, and regime III corresponds to an oscillation from 0 to u^*. Lower panel: Dashed arrows indicate the trajectory of the surface into the N, L_0 plane. The dotted line indicates the continuous steady state, and solid line indicates the discontinuous steady state.

is more accurate. Good agreement with the full step model is also found in regime II, as shown in Fig. 3. (iii) The scaling of the smallest terrace size at 1250 °C was confirmed experimentally in Ref. [16]. Using their result $l_{\min} \approx N^{-2/3} \times 10^2$ nm, and assuming slow kinetics $d \ll \bar{\rho}^{-1}$ as suggested by Ref. [9], we extract $\xi \approx 10^7$ nm,

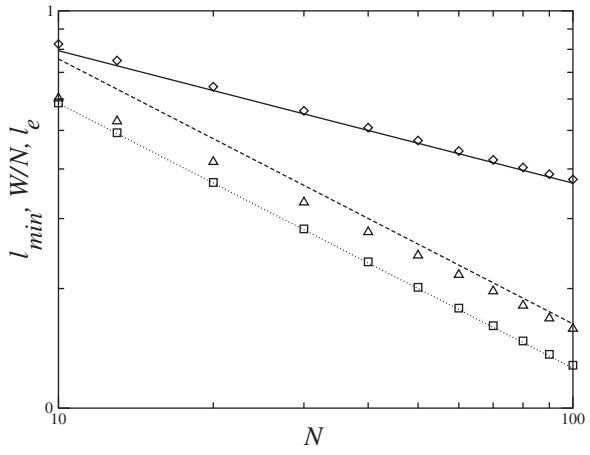

FIG. 3. Analysis of one bunch in regime II. The parameters are $d = 0.1$, $\xi = 500$, and $A = 0.001$. The lines indicates the analytical prediction of regime II. The squares, triangles, and diamonds, represent numerical results for $L_{\min}$, W/N, and L_e, respectively. These results are found for a periodic box size of $L_{\text{box}} = 5000$, but do not depend on L_{box} as long as $L_{\text{box}} \gg \xi$.

which leads to an effective charge of ≈ 0.02 electronic charge. (iv) The dynamics follow the path presented on Fig. 2. Assuming the relevance of a unique lengthscale $N \sim t^{\beta}$ only, and that the flux scales as $j \sim N^{-\delta}$, and using the additional constraints of constant slope, together with mass conservation, we obtain $j(y, t) = t^{-\delta\beta}\mathcal{J}(y/t^{\beta})$, and $x(y, t) = t^{\beta}\chi(y/t^{\beta})$, where $\mathcal{J}$ and χ are unknown functions. Substituting into mass conservation $\partial_t x = -\partial_y j$, we find $\beta = 1/(2 + \delta)$. We recover the result of Liu and Weeks [9] in the limit $\delta = 0$, which is in agreement with the experiments of electromigration on Si(111) [17]. In the large bunch limit, a different scaling is found $\delta = 1/2$ and $\beta = 2/5$. (v) Let us mention finally that in the light of the present discussion, care must be taken regarding a phenomenological study of bunching since the assumption of a unique regime [18] no longer holds. This is further corroborated by a recent analysis of step bunching during growth in the presence of an inverted Schwoebel effect. There, two different steady-state regimes were identified [7]. Since many steps run between bunches during growth, the dynamics is quite different from ours, however. Indeed, the separation of the bunches, with wide terraces (which are free of steps) does not occur during growth.

[1] A. V. Latyshev *et al.*, Surf. Sci. **213**, 157 (1989).
[2] H.-C. Jeong and E. D. Williams, Surf. Sci. Rep. **34**, 171 (1999); M. Degawa *et al.*, J. Phys. Soc. Jpn. **70**, 1026 (2001).
[3] M. Sato and M. Uwaha, Europhys. Lett. **32**, 639 (1995); C. Misbah and O. Pierre-Louis, Phys. Rev. E **53**, R4318 (1996).
[4] M. Sato and M. Uwaha, Surf. Sci. **442**, 318 (1999).
[5] J.-J. Métois and S. Stoyanov, Surf. Sci. **440**, 407 (1999).
[6] D. Kandel and J. D. Weeks, Phys. Rev. Lett. **72**, 1678 (1994).
[7] J. Krug, V. Tonchev, S. Stoyanov, and A. Pimpinelli, Phys. Rev. B **71**, 045412 (2005); V. Popkov and J. Krug, Europhys. Lett. **72**, 1025 (2005).
[8] O. Pierre-Louis and J.-J. Métois, Phys. Rev. Lett. **93**, 165901 (2004).
[9] D.-J. Liu and J. D. Weeks, Phys. Rev. B **57**, 14 891 (1998).
[10] S. Stoyanov, Jpn. J. Appl. Phys. **30**, 1 (1991).
[11] J.-J. Métois *et al.*, Nat. Mater. **4**, 238 (2005).
[12] O. Pierre-Louis *et al.*, Phys. Rev. Lett. **80**, 4221 (1998).
[13] F. Gillet, O. Pierre-Louis, and C. Misbah, Eur. Phys. J. B **18**, 519 (2000); O. Pierre-Louis, Europhys. Lett. **72**, 894 (2005).
[14] P. Politi and C. Misbah, Phys. Rev. Lett. **92**, 090601 (2004).
[15] S. Stoyanov and V. Tonchev, Phys. Rev. B **58**, 1590 (1998).
[16] K. Fujita, M. Ichikawa, and S. Stoyanov, Phys. Rev. B **60**, 16 006 (1999).
[17] N.-Y. Yang, E. S. Fu, and E. D. Williams, Surf. Sci. **385**, 101 (1996).
[18] A. Pimpinelli *et al.*, Phys. Rev. Lett. **88**, 206103 (2002).